

Experimental Confirmation of Kelvin's Equilibria

Georgios H. Vatistas,* Hamid A. Abderrahmane, and M. H. Kamran Siddiqui

Department of Mechanical and Industrial Engineering, Concordia University, Montreal H3G 1M8, Canada

(Received 25 October 2007; published 30 April 2008)

We experimentally corroborate the core analytical deductions of Thomson's 124-year-old theorem, *vis-à-vis* the stability of a ring of N vortices. Observations made in water vortices produced inside a cylinder via a revolving disk confirm that the regular N -gons are stable for $N \leq 6$ and unstable for $N \geq 8$. The $N \leq 6$ equilibria are exceptionally resilient. When destroyed, they reemerge in their original form. We reason that the heptagonal system either survives in an exceedingly narrow band of disk speeds or is in theory critically stable. Contrary to the results with a rotating bottom reported by Jansson *et al.* [Phys. Rev. Lett. **96**, 174502 (2006)], we show the interfacial axial symmetry does not break spontaneously but through spectral development, the functional relationship amongst the polygon rotation and disk speed is surprisingly simple, and the pattern to disk frequency ratio depends on both Froude and wave numbers.

DOI: [10.1103/PhysRevLett.100.174503](https://doi.org/10.1103/PhysRevLett.100.174503)

PACS numbers: 47.32.-y

Whirlpools produced in simple confinements have been employed to elaborate on some fundamental properties of rotating flows. Yarmchuk, Gordon, and Packard [1] disclosed the existence of quantized stationary vortex arrays in a rotating cylindrical pail containing superfluid ^4He below the λ point. Vettin [2] employed a rotating dish with a centrally located cylindrical cup filled with ice to simulate Earth's polar circulation. Fridman *et al.* [3] examined the role of centrifugal instability in the development of the spiral structure of spiral galaxies in a stationary dish with a rotating ring or conical cuplike device. In the latter part of the 1980s during detailed mappings of the free-surface elevation of liquid vortices [4], the first author came across an unexpected interfacial symmetry breaking of a liquid vortex produced in a cylinder via a rotating disk near the bottom. The experience, among other captivating manifestations, was reported in a series of articles [5–8]. A recent letter by Jansson *et al.* [9] triggered a rejuvenated interest in the previous discovery [5]. The fundamental significance of the event in several scientific and technological disciplines [5,9–11] was the cause behind the ensued hype. Among the areas where this phenomenon appears to be pertinent are atmospheric sciences. Near the polar region, the Earth's surface is disklike while the atmosphere above has an "interface." Notwithstanding the added complexities associated with large-scale geophysical vortices, the close resemblance amongst the observed regular polygonlike free-surface shapes and the weather patterns in Antarctica [12] is intriguing. Additionally, satellite images of the eyewall of hurricanes Betsy and Anita [13] unveil indisputably polygonal structures.

Swirling flows are susceptible to instabilities that often lead to phenomena such as the roll up of vorticity filament into vortices via the Kelvin-Helmholtz instability, merging of vortices, or the emergence of vortex equilibrium patterns termed "point vortices." The theoretical work on the last topic was started by Lord Kelvin [14], who in 1878 solved the case of three vortices in connection with the now

abandoned theory of vortex atoms. In 1883 Thomson [15] dealt with the cases of three, four, five, six, and seven vortices, where he predicted instability to occur for seven vortices. Havelock [16] generalized the approach to N vortices, showing that, with no boundary, the case of seven vortices was neutrally stable, and unstable in the presence of confining outer or inner boundaries. He also considered the occurrence of N vortices arranged in a ring with a fixed central vortex and demonstrated that a sufficiently strong central vortex could stabilize an otherwise unstable ring. Dhanak [17] theoretically demonstrated that vortex systems with small but finite cores pose the same stability characteristics, with $N = 7$ being unstable to only one normal mode of disturbance. Dritschel [18] had found earlier that $N = 7$ was unstable to two displacement type of modes. All the linear analytical approaches of the past were partial and thus dubious for the case of seven point vortices. Recently, based on the nonlinear Kirchhoff equation, Kurakin and Yudovich [19] confirmed that the $N \leq 6$ and $N \geq 8$ states are stable and unstable, respectively. Furthermore, they also proved the seven-vortex array to be stable in theory. It is interesting to note that the theoretical derivation for the stability of point vortices has its foundation in the analogy between point vortices and point masses, whereby the vortex strength is replaced by the mass. The previous theoretical models are idealizations of our experiments when the liquid height is low.

In the experimental side, Yarmchuk, Gordon, and Packard [1] showed that two-dimensional stable vortex patterns could evolve in ^4He as the superfluid constituent interacts with the normal fluid component. They were, however, unable to test directly the stability of the observed configurations. The equations describing strongly magnetized electron columns and those describing two-dimensional Eulerian flows are dual. Because of the latter dynamic similarity, electron columns in a Malmberg-Penning trap and ring vortices should evolve identically. Based on this analogy Durkin and Fajans [20] were able to

confirm the key theoretical predictions of Havelock [16]. Until recently, however, no direct experimental validation of the phenomenon has been made in a normal fluid flow.

In this Letter we experimentally confirm directly the basic conclusions of the venerable theory [14,15], expand and elaborate on some key attributes of the phenomenon, and finally report on new developments associated with the event.

The present tests were conducted using the apparatus shown in Fig. 1(a). A CCD camera was placed on top of the cylinder to image the hollow-core vortex formed on the disk. The camera acquired a sequence of images for each mode at a rate of 30 frames per second as 8-bit gray-scale images. The rotary motion imparted to the fluid by the disk generates a centrifugal force field and pushes the liquid towards the reservoir's wall, developing a depression near the axis of rotation. As the speed of the rotating disk reaches a specific value the water surface touches the disk and the line intersection between the liquid, air, and the surface of disk outlines the core shape. Contrary to the intuitively expected circular dry spot, the core starts to develop different polygonal shapes; see, for example, Fig. 1(b).

Previously [5–8] the N patterns were determined by visual inspection using a stroboscope. The different polygons and their speed of rotation are now identified and measured via image processing. The boundary of the pattern is extracted using the segmentation technique applied on the binary images. The speed of the pattern is accurately determined using power spectrum analysis of the time series of the radius of a given point on the pattern bound-

ary. The speed of the disc is measured by the image juxtaposition of two marks on the disk.

Jansson *et al.* [9] reported that “the shape of the free surface can spontaneously break the axial symmetry.” They found the rotation rate of the free-surface polygons to vary with the disk speed “in a complicated way.” Their tests were made with $\sigma(R_d/R_t) \sim 1$, where R_d and R_t are the disk and tank radii, respectively. Our recent verifications using a disk diameter almost equal to the container validate this ill-defined symmetry breaking. However, with $\sigma = 0.824, 0.887, \text{ and } 0.944$, the polygonal core shapes evolve gradually and in succession, separated by a gap of mixed states in between. For exceedingly low rotational disk speeds (ω_d), the vortex core remains circular ($N = 0$). Increasing its rotation, the flow transfers into another state characterized by a precessing circular core ($N = 1$). A further increase of the disk speed progressively yields cores with “ellipsoidal” ($N = 2$), triangular ($N = 3$), square ($N = 4$), pentagonal ($N = 5$), and hexagonal ($N = 6$) cross sections. Typical images of the actual equilibria (with $2 \leq N \leq 6$) are given in Fig. 1(b). As the disk speed increases beyond the $N = 6$ state, a continuous amplification of dynamical noise eventually wipes out the sharp spectral peaks. A typical spectrum of the stationary and mixed-mode states is shown in Fig. 2(a). Within a specific equilibrium state the wave celerity increases linearly with the disk speed [6]. In the beginning of the stationary state interval, the sides of the pattern curve inwards [Fig. 2(b), (i) & (ii) and (iv) & (v)]. As the disk picks up speed, the sides of the polygon flatten out, producing a fuller shape. The equilibrium polygons are exceptionally stable. When disturbed or even completely destroyed (by inserting a solid rod into the flow), the patterns reemerge after a short period of time almost in their original form. The last suggests that this phenomenon is not particularly sensitive to initial conditions. Note that a small degree of hysteresis (of $\sim 4\%$) exists [8]. The transition between two stationary states happens in a surprisingly straightforward manner. The gap between neighboring equilibria is inhabited by mixed-mode states. For example, between the $N = 3$ and $N = 4$ interval [Fig. 2(b), (iii)], the core consists from the superposition of waves from the adjoining equilibria. Close to the N state the N wave dominates, while close to the opposite side the $N + 1$ wave takes over. Because the two have different phase speeds the core is not stationary. As the disk speed increases from $N = 3$ towards $N = 4$ [Fig. 2(b)], one of the lobes grows fatter mutating afterwards into two, thus providing the required extra lobe to form the neighboring state [Fig. 2(b), (iv) & (v)].

In our previous exploratory experiments, visual inspection using a water-soluble dye revealed that the patterns were present even if the core was flooded. Recent higher fidelity images shown in Fig. 2(c) confirm the old observation. Near the core, a “circular” dry spot exists. However, the region where the apexes of the polygon are located is flooded with water. The light coloring at the polygon tips indicates a free-surface depression. The last is

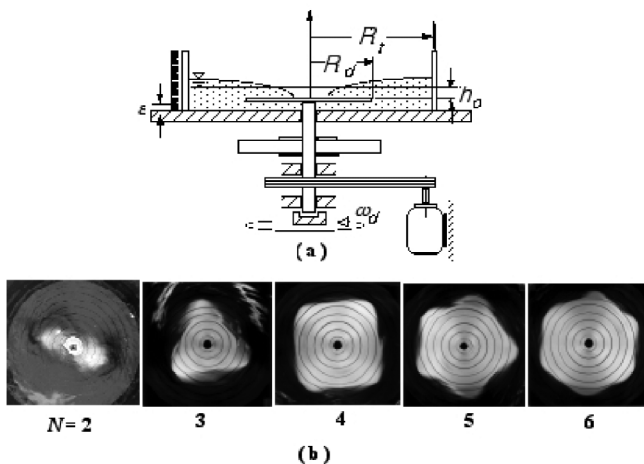
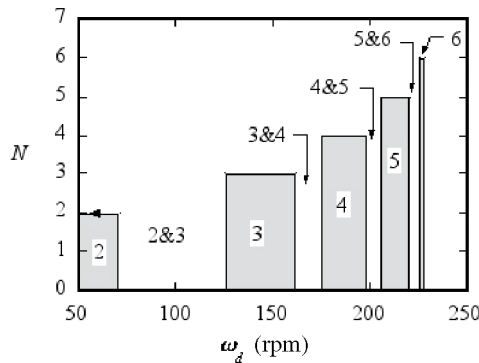
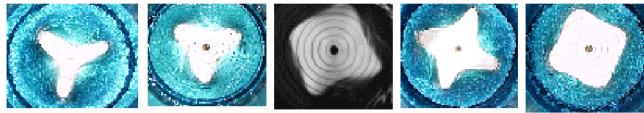


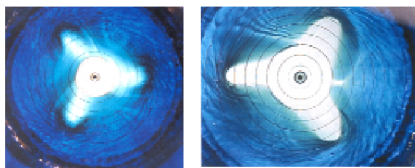
FIG. 1. (a) Schematic of the experimental apparatus. The present experiments were conducted using tap water in a 284 mm diameter stationary cylindrical container with a 252 mm diameter circular disk spinning near the bottom. A variable-speed electrical motor drives the disk. The initial water level was measured using a ruler attached to the side of the tank. Three different initial liquid heights (20, 25 and 30 mm) were used in the present experiments; (b) typical equilibria of $N = 2, 3, 4, 5, \text{ and } 6$.



(a)



(b)



(c)

(d)

FIG. 2 (color online). (a) A typical equilibrium and mixed-mode gaps spectrum for $h_o = 25$ mm. The bandwidth of both the equilibrium and mixed modes become narrower with the wave number N . (b) Changes in the polygonal structure within the $N = 3$ (i & ii) and 4 (iv & v) states. In the beginning of the stationary state interval, the sides of the pattern curve inwards. As the disk speed increases, the sides of the polygon flatten out producing a fuller shape, (iii) typical mixed-mode state whereby the core consists from the superposition of both fundamental frequency waves $N = 3$ and 4. The centrifugal force pushed the liquid outwards. The retreating liquid exposes the structure of the core. Every vortex with an interface develops a free-surface depression near the axis of rotation. On the apexes of the polygonal core shapes, satellite vortices exist. Each satellite vortex possesses a dimple, very evident by the faded color of the flooded polygon tips in (c), indicating the presence a free-surface depression due to the satellite vortex. Since the parent vortex is stronger, the central portion is dry. When the rotation intensifies, both parent and satellite vortices become stronger. The receding water develops lobes in the place where the secondary vortices existed, and thus forms the dry polygonal central pattern (d).

due to the local centrifugal force generated by the satellite vortices orbiting the central vortex. In their experiments with ethylene glycol, Jansson *et al.* [9] described clearly the presence of “spiraling vortices on top of the polygon structure.” Furthermore, the numerical simulations of Miraghaie, Lopez, and Hirska [21] for $N = 3$ in shallow depth show indisputably the presence of three vortices located at the apexes of the regular triangle. When the rotation intensifies, both parent and satellite vortices become stronger. The receding water develops lobes in the

place where the secondary vortices existed, and thus forms the dry polygonal central pattern shown in Fig. 2(d). Because of the added radial thrust a free-surface upwelling near the cylindrical wall, where these vortices are positioned, is noticeable. Hence, the polygonal shapes can be viewed as either waves inside the main vortex or ensembles of satellite vortices located at the corners of a polygon attached to the parent vortex, rotating in unison at a constant speed. In other words, when a liquid is the working fluid, the manifestation displays a vortex-wave duality.

It is pleasing to find the main predicted stability characteristics of the ideal problem [14–16] to be ingrained in the real phenomenon. Thus our observations reveal that all systems with $N \leq 6$ vortices located in the vertices of regular polygons, arranged in a circular row, with an exterior boundary, under the presence of a strong central vortex, are stable. The $N \geq 8$ ensembles are unstable and hence undetectable. Despite the repeated extra care taken to isolate all the vibrations in the experimental apparatus, we were also unable to produce the $N = 7$ case. Jansson *et al.* [9] were also able to produce only polygons up to $N = 6$. Closely examining the equilibrium spectrum [see Fig. 2(a)], we notice that the interval of the survival of the states decreases with the wave number. For $N = 6$ the equilibrium lasts within the interval [225, 228] rpm. Therefore, if $N = 7$ exists, it must either live in an exceedingly narrow range of disk speeds or it is in theory critically stable. Because in real settings the problem is infested by

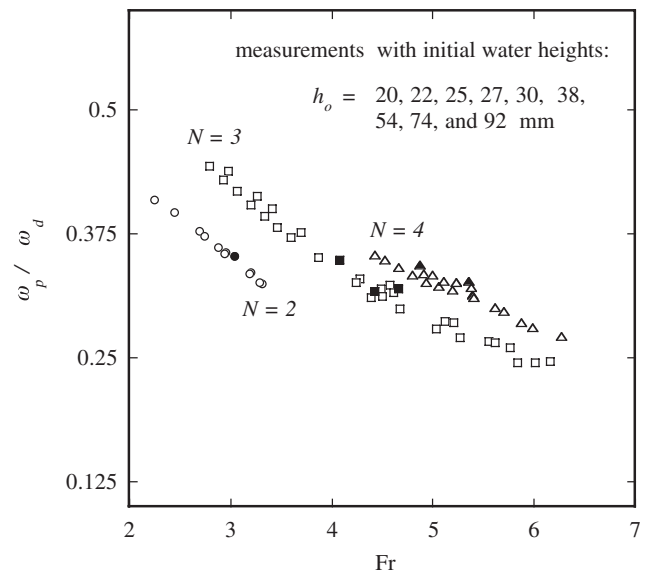


FIG. 3. Dependency of the frequency ratio on the Froude and wave numbers ($R_d = 126$ mm), where $Fr = \omega_d R_d / \sqrt{g \cdot h_o}$, and g is the gravitational constant. Note that Buckingham’s π theorem for the problem under consideration leads to $\omega_p / \omega_d = \{N, Fr, h_o / R_d, R_d / R\}$. Two sets of data are presented. For the first, the pattern speed (open geometric shapes) was determined manually, while for the second (solid geometric shapes) through image processing.

various types of internal and external disturbances, if the $N = 7$ system is critically stable, it will not appear.

According to one of Havelock's [16] corollaries, the point vortices should stabilize on rings of about half the radius of the containing vessel. Our present tests with h_o ranging from 20 to 30 mm and those of [9] show that the equilibrium patterns (with N higher than 2) are inscribed within a circle having a radius of approximately half of the container radius.

In all past and present experimental trials, the polygonal shapes were found to rotate at a slower speed than the disk. For the current tests, where $\sigma = 0.887$, three different heights, and for all stable N -gons (including $N = 2$), the frequency ratio ω_p/ω_d (where ω_p and ω_d are the speeds of the pattern and disk, respectively) was found to decrease with the Froude number and increases with the wave number N ; see, for example, Fig. 3. The last does not correspond to $2/3$ for $N = 2$, nor to the $\omega_p/\omega_d = 1/N$ for $3 \leq N \leq 6$ as suggested in [9].

As we were finalizing this article, some supplementary events requiring further attention have surfaced. Processing the images, in addition to the fundamental N wave (for $2 \leq N \leq 6$), we have detected harmonic waves with $2N$, $3N$, $4N$, $5N$, etc., that are encircling the basic pattern. In an expanded forthcoming paper, we are planning to examine the attributes of this manifestation in detail.

*Corresponding author.

vatistas@encs.concordia.ca

- [1] E. J. Yarmchuk, M. J. V. Gordon, and R. Packard, Phys. Rev. Lett. **43**, 214 (1979).

- [2] F. Vettin, Ann. Phys. (Leipzig) **102**, 246 (1857).
 [3] A. M. Fridman, A. G. Morozov, M. V. Nezhlin, and E. N. Snezhkin, Phys. Lett. **109A**, 228 (1985).
 [4] G. H. Vatistas, J. Hydraul. Res. **27**, 417 (1989).
 [5] G. H. Vatistas, J. Fluid Mech. **217**, 241 (1990).
 [6] G. H. Vatistas, J. Wang, and S. Lin, Exp. Fluids **13**, 377 (1992).
 [7] G. H. Vatistas, J. Wang, and S. Lin, Acta Mech. **103**, 89 (1994).
 [8] G. H. Vatistas, N. Esmail, and C. Ravanis, AIAA Paper No. AIAA 2001-0168, 2001.
 [9] R. N. Jansson, M. P. Haspang, K. H. Jensen, P. Hersen, and T. Bohr, Phys. Rev. Lett. **96**, 174502 (2006).
 [10] R. N. Jansson, M. P. Haspang, K. H. Jensen, P. Hersen, and T. Bohr, Phys. Rev. Lett. **96**, 174502 (2006); **98**, 049901(E) (2007).
 [11] H. Aref and D. L. Vainchtein, Nature (London) **392**, 769 (1998).
 [12] S. M. O'Carroll and R. J. Gutro, "The Antarctic Ozone Hole," Poster paper, American Geophysical Union Fall 2002 Meeting in the Moscone Convention Center, 6 December 2002 (unpublished).
 [13] B. M. Lewis and H. F. Hawkins, Bull. Am. Meteorol. Soc. **63**, 1294 (1982).
 [14] W. Thomson (Lord Kelvin), *Mathematical and Physical Papers* (Cambridge University Press, Cambridge, England, 1878), Vol. IV, p. 135.
 [15] J. J. Thomson, *Treatise on Vortex Rings* (Macmillan, London, 1883), p. 94.
 [16] T. H. Havelock, Philos. Mag. **11**, 617 (1931).
 [17] M. R. Dhanak, J. Fluid Mech. **234**, 297 (1992).
 [18] D. G. Dritschel, J. Fluid Mech. **157**, 95 (1985).
 [19] L. G. Kurakin and V. I. Yudovich, Chaos **12**, 574 (2002).
 [20] D. Durkin and J. Fajans, Phys. Fluids **12**, 289 (2000).
 [21] R. Miraghaie, J. M. Lopez, and A. H. Hirska, Phys. Fluids **15**, L45 (2003).